Comment on "Test of the Stark-effect theory using photoionization microscopy"

P. Giannakeas,* F. Robicheaux,† and Chris H. Greene‡
Department of Physics and Astronomy, Purdue University, West Lafayette, Indiana 47907, USA
(Received 12 November 2014; published 3 June 2015)

An article by Zhao *et al.* [Phys. Rev. A **86**, 053413 (2012)] tests the local frame transformation (LFT) theory by comparing it with benchmark coupled-channel calculations. The system under consideration is an alkali-metal atom that is two-photon ionized in the presence of a static external electric field. Zhao *et al.* state that the differential cross sections computed in the LFT theory disagree with their supposedly more accurate coupled-channel calculations. They went on to diagnose the discrepancy and claimed that it originates in an inaccurate correspondence between the irregular functions in spherical and parabolic-cylindrical coordinates, a correspondence that lies at the heart of LFT theory. We have repeated the same tests and find that our calculations rule out the discrepancies that were claimed in Zhao *et al.* [Phys. Rev. A **86**, 053413 (2012)] to exist between the LFT approximation and the exact calculations. This Comment thus helps to clarify the accuracy of the Harmin-Fano theory and demonstrates that it is in fact remarkably accurate not only for the total photoionization cross section in the Stark effect, but also for the differential cross section in photoionization microscopy.

DOI: 10.1103/PhysRevA.91.067401 PACS number(s): 32.80.Fb, 07.81.+a

I. INTRODUCTION

The Stark-effect theory for nonhydrogenic atoms was formulated by Harmin [1–3] and Fano [4], and it was an impressive breakthrough that enabled the quantitative interpretation of both resonant and nonresonant photoabsorption spectra. One of the main points of the Harmin-Fano theory lies in the fact that the scattering observables at long electron distances can be interconnected with the scattering information, such as quantum defects determined at short distances. This is permitted because the Coulomb-Stark Schrödinger equation is separable over a large range of electron distances in *both* spherical coordinates (r,θ,ϕ) and parabolic-cylindrical coordinates (ξ,η,ϕ). For example, for an electric field of strength 1 kV/cm this range is identified to be at least 50 atomic units. The interrelation is achieved by means of a local frame transformation (LFT) at distances far shorter than Stark's barrier maximum, i.e., $r \ll F^{-1/2}$ where F is the field strength and r is the separation distance. In this manner, the LFT allows the mapping of the regular and irregular solutions from spherical to parabolic-cylindrical coordinates [4]. Specifically, the regular solutions between the two coordinate systems obey the following relations:

$$\frac{f_{\epsilon\ell m}(\mathbf{r})}{r} = \sum_{n_1} \psi^{\epsilon F}_{n_1 m}(\mathbf{r})[(\underline{U}^T)^{-1}]^{\epsilon F m}_{n_1\ell} \quad \text{for} \quad r \ll F^{-1/2}, \quad (1)$$

where ℓ and m indicate the orbital and azimuthal angular momentum quanta, respectively. The index n_1 labels successive eigenstates of the fractional charge β_{n_1} and is essentially the number of nodes in the up-field parabolic-cylindrical coordinate ξ (see Eq. (3a) in Ref. [1]). The crucial quantity $[(\underline{U}^T)^{-1}]^{\epsilon F m}_{n_1\ell}$ is a matrix element of the local frame transformation where ϵ denotes the energy and F is the strength of the electric field. $f_{\epsilon\ell m}(\mathbf{r})r^{-1}$ are the regular solutions in spherical coordinates which vanish at the origin, and they correspond to the Coulombic regular functions. Similarly, the term $\psi^{\epsilon F}_{n_1 m}(\mathbf{r})$ represents the regular functions in parabolic-cylindrical coordinates.

On the other hand the mapping of the irregular solutions reads

$$\frac{g_{\epsilon\ell m}(\mathbf{r})}{r} = \sum_{n_1} \chi^{\epsilon F}_{n_1 m}(\mathbf{r}) \csc(\gamma_{n_1})(\underline{U})^{\epsilon F m}_{n_1\ell} \quad \text{for} \quad r \ll F^{-1/2}, \quad (2)$$

where $g_{\epsilon\ell m}(\mathbf{r})r^{-1}$ is the irregular function in spherical coordinates and it essentially corresponds to the irregular Coulomb function which lags the regular solution by $\pi/2$ at short distances $r \ll F^{-1/2}$. Note that this Eq. (2) coincides with Eq. (20) of Ref. [5], except that the notation has been revised to agree with that of Ref. [1] where this formula was initially derived. Here γ_{n_1} indicates the phase that the electron's wave function has accumulated before and through the Stark barrier in the down-field coordinate η. The factor $\csc(\gamma_{n_1})$ ensures that the right-hand side (RHS) of Eq. (2) has the same energy normalization amplitude at small r as the irregular Coulomb function (see the discussion of Eq. (48) in Ref. [1]).

Equations (1) and (2) are the key parts of the LFT theory, and they permit the asymptotic scattering observables to be expressed in terms of the photoabsorption dipole amplitudes determined close to the origin. Having clarified and briefly reviewed the key concepts of LFT theory, the following section focuses on the claims of Ref. [5].

II. COMMENT

In Ref. [5] Zhao *et al.* [5] observe noticeable discrepancies between Harmin's LFT theory for the Stark effect of alkali atoms [1–3] and the presumably accurate coupled-channel theory in their calculations of the differential cross sections for the two-photon π-polarized ionization process of Na atoms in the presence of a uniform electric field. These discrepancies were then claimed by Zhao *et al.* [5] to originate in an erroneous mapping of the irregular functions Eq. (2) from one coordinate system to another.

*pgiannak@purdue.edu
†robichf@purdue.edu
‡chgreene@purdue.edu

Because Zhao *et al.* [5] raise serious criticisms of the LFT theory, it is important to further test their claims of error and their interpretation of the sources of error. Their contentions can be summarized as follows:

(i) The Harmin-Fano LFT accurately describes the total photoionization cross section, but it has significant errors in its prediction of the differential cross section that would be measured in a photoionization microscopy experiment. They deduced this by comparing the results from the approximate LFT with a numerical calculation that those authors regard as essentially exact.

(ii) The errors are claimed to be greatest when the atomic quantum defects are large and almost negligible for an atom, such as hydrogen which has vanishing quantum defects. They then present evidence that they have identified the source of those errors in the LFT theory, namely, the procedure first identified by Fano that predicts how the irregular spherical solution evolves at long distances into parabolic coordinate solutions. Their calculations are claimed to suggest that the local frame transformation of the solution, regular at the origin from spherical to parabolic coordinates [see Eq. (1)], is correctly described by the LFT, but the irregular solution transformation is incorrect [see Eq. (2)].

Here we reinvestigate the main points of Ref. [5] with the Harmin-Fano LFT and present evidence that both of their claims are erroneous.

III. RESULTS AND DISCUSSION

Consider the differential cross section of photoionization microscopy as shown in Fig. 1 as a function of the cylindrical coordinate ρ that is transverse to the applied field direction. This example refers to the two-photon π-polarized ionization process of Na atoms in the presence of an external electric field for parameters of the case addressed in Fig. 1 of Ref. [5]. The first pulse excites a ground-state Na atom into the $3p$ orbital, and the second pulse excites the valence electron up to a high Rydberg state energy. The strength of the field is $F = 3590$ V/cm, the energy is $\epsilon = -62$ cm^{-1}, and the detector is placed at $z_{\rm det} = -1$ mm. The red solid line refers to the LFT results calculated within the R-matrix framework, and the black dots denote the *ab initio* numerical solution of the time-dependent Schrödinger equation through a "velocity mapping" technique (for further details see Ref. [6]). Figure 1(a) includes coherent contributions from the dipole transitions $3s \to 3p \to \epsilon s$ and $3s \to 3p \to \epsilon d$ orbitals with an intermediate azimuthal angular momentum $m_{\rm int} = 0$ to a final $m_f = 0$. Figure 1(b) corresponds instead to the dipole transitions from the $3s \to 3p \to \epsilon d$ orbital with $m_{\rm int} = 1$ to $m_f = 1$. Note that the atomic fine structure has been neglected here and in the corresponding study by Zhao *et al.*

Clearly, our LFT and numerical calculations are in excellent agreement, which contradicts the disagreement found by Ref. [5]. In fact, our calculations agree well with the LFT calculations of Zhao *et al.* as can be seen in the corresponding panels in Fig. 1 of Ref. [5] (within an overall normalization factor). Interestingly, in panel (a) of Fig. 1 our LFT (red solid line) agrees with our numerical results (black dots). Hence, the disagreement observed by the Zhao *et al.* originates from errors in those authors' coupled-channel calculations and not from

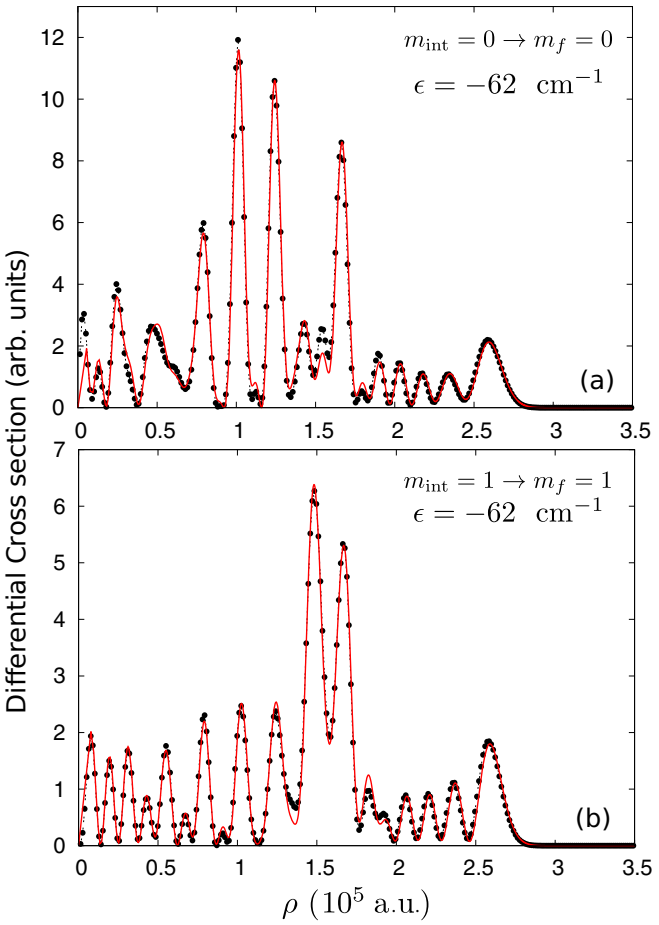

FIG. 1. (Color online) The differential cross section for photoionization microscopy of a Na atom is shown as a function of the cylindrical coordinate ρ. The red solid lines indicate the LFT theory calculations, whereas the black dots denote the velocity mapping results from our direct solution of the two-dimensional inhomogeneous Schrödinger equation. Panels (a) and (b) refer to energy $\epsilon = -62$ cm^{-1} for the transitions $m_{\rm int} = 0 \to m_f = 0$ and $m_{\rm int} = 1 \to m_f = 1$, respectively. In all cases the field strength is $F = 3590$ V/cm, and the detector is placed at $z_{\rm det} = -1$ mm. Note the excellent agreement that is evident between the LFT calculation and the accurate full numerical treatment, which contrasts with the poor agreement for the same parameters that was observed in the calculations shown in Fig. 1 of Ref. [5].

inaccuracies of the LFT mapping of the irregular functions from spherical to parabolic coordinates [see Eq. (2)].

Indeed, Figs. 5(b) and 5(c) of Zhao *et al.* document their contention that the left and right sides of Eq. (2) are not even approximately equal. We have repeated those calculations for identical choices of field strength, energy, and quantum numbers, and our results give evidence that if the summation on the RHS of Eq. (2) is converged, the equation is satisfied accurately.

Figure 2 compares the analytically known irregular Coulomb function $g^{(C)}_{\epsilon\ell m}(\mathbf{r})r^{-1}$ (black solid line) with the corresponding frame-transformed-(FT-) irregular function $g^{(\rm LFT)}_{\epsilon\ell m}(\mathbf{r})r^{-1}$ (red dots) at energy $\epsilon = -135.8231$ cm^{-1} [7] and field strength $F = 640$ V/cm. Both irregular functions

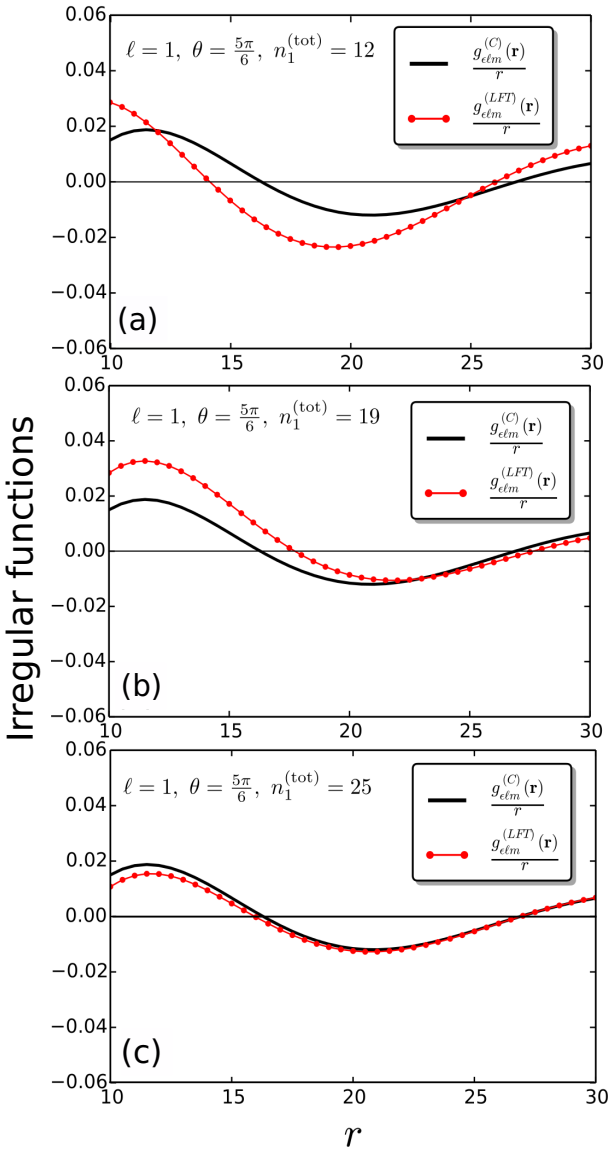

FIG. 2. (Color online) The irregular solutions in spherical coordinates at negative energies, i.e., $E = -135.8231\ \mathrm{cm}^{-1}$, illustrated for $\mathbf{r} = (r,\theta = \frac{5\pi}{6},\phi = 0)$. In all panels the orbital angular momentum and the azimuthal quantum number are set to be $\ell = 1$, $m = 1$, and the black solid line indicates the analytically known irregular Coulomb function, namely, $g^{(C)}_{\epsilon\ell m}(\mathbf{r})r^{-1}$. Accordingly, the red dots correspond to the LFT calculations of the irregular function, namely, $g^{(\mathrm{LFT})}_{\epsilon\ell m}(\mathbf{r})r^{-1}$. Panels (a)–(c) depict the LFT calculations for a maximum number of n_1 states equal to $n_1^{(\mathrm{tot})} = 12$, 19, and 25, respectively. All the $n_1^{(\mathrm{tot})}$ correspond to $\beta_{n_1} < 1$.

are expressed in spherical coordinates with angles being fixed according to the expression $\mathbf{r} = (r,\theta = \frac{5\pi}{6},\phi = 0)$. In addition, the orbital and azimuthal angular momentum are set to be $\ell = 1$, and $m = 1$. These are the same as in Fig. 5(b) of Ref. [5].

In Fig. 2 panels (a)–(c) correspond to the FT-irregular function with different total numbers of n_1 states included in the sum of Eq. (2). More specifically, panels (a)–(c) refer to a total number of n_1 states equal to $n_1^{(\mathrm{tot})} = 12$, 19, and 25, respectively. Notice that for an increasing number of n_1 states the FT-irregular function (red dots) converges better and better to the corresponding Coulomb irregular function (black solid line). Specifically, panel (c) shows excellent agreement, and the correct nodal pattern is predicted. Our panel (c) does not exhibit the discrepancies presented in the corresponding Fig. 5(b) of Zhao *et al.* Ref. [5].

A major conclusion here is that the convergence criteria of Ref. [5] in Fig. 5(b) are not sufficient since Fig. 2 implies that one must in general consider all the n_1 states that fulfill the relation of $\beta_{n_1} < 1$, i.e., $n_1^{(\mathrm{tot})} = 25$ for this case and not only a few of them. Analysis of the RHS of Eq. (2) shows that the frame transformation matrix elements $U^{\epsilon Fm}_{n_1\ell}$ decrease rapidly for $n_1 \geqslant 7$ (i.e., $U^{\epsilon Fm}_{n_1=15,\ell} = -1.5236\times10^{-22}$). This behavior arises from the amplitude $1/R_{n_1}$ of the regular function of the down-field degree of freedom which vanishes due to tunneling under the Stark barrier (i.e., $1/R_{n_1=15} = 6.3946\times10^{-22}$). Furthermore, the amplitude $1/S_{n_1}$ of the χ-parabolic irregular functions in Eq. (2) for $n_1 \geqslant 7$ vanishes as well (i.e., for $1/S_{n_1=15} = 3.3501\times10^{-22}$). Note that here we strictly follow the notation of Ref. [1]. On the other hand the quantity $\csc(\gamma_{n_1}) = R_{n_1}S_{n_1}$ (see Eq. (47) in Ref. [1]) rapidly increases for $n_1 \geqslant 7$ (i.e., $\csc\ \gamma_{n_1=15} = 4.6678\times10^{42}$). Therefore, on the RHS of Eq. (2) the quantities, $1/R_{n_1}$, $1/S_{n_1}$, and $\csc\ \gamma_{n_1}$ simplify yielding nonvanishing matrix elements for all the n_1 states with $\beta_{n_1} < 1$. The calculations of these quantities are based on R-matrix eigenchannel theory (see Ref. [6]). This quantitative analysis shows that photoabsorption observables rapidly converge as n_1 is increased mainly due to the amplitudes $1/R_{n_1}$, whereas the frame-transformed irregular function converges far more slowly.

For almost all applications, the states with $\beta_{n_1} < 1$ are the physically relevant ones since they correspond to an attractive Coulomb potential in the down-field degree of freedom η. Only for these states can the wave function probe the ionic core, which represents the only part of the Hamiltonian that couples the different n_1 parabolic channels. On the other hand the states for $\beta_{n_1} > 1$ correspond to a repulsive Coulomb potential in the η degree of freedom, that effectively shields the ionic core.

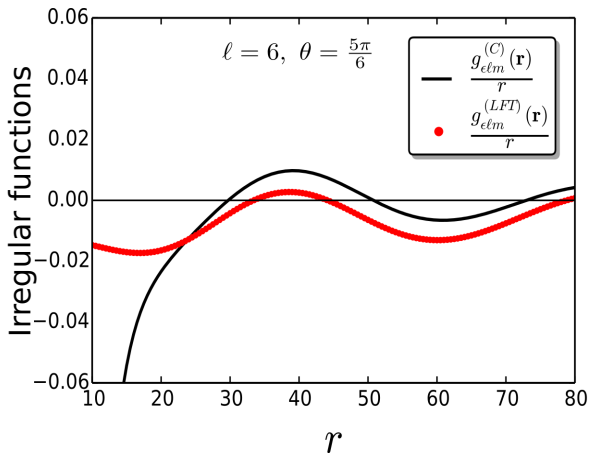

FIG. 3. (Color online) The irregular solutions in spherical coordinates at a negative energy, namely, $E = -135.8231\ \mathrm{cm}^{-1}$, illustrated for $\mathbf{r} = (r,\theta = \frac{5\pi}{6},\phi = 0)$ and $\ell = 6$, $m = 1$. The black solid line indicates the analytically known irregular Coulomb function, namely, $g^{(C)}_{\epsilon\ell m}(\mathbf{r})r^{-1}$, and the red dots correspond to the FT-irregular function, namely, $g^{(\mathrm{LFT})}_{\epsilon\ell m}(\mathbf{r})r^{-1}$. In the LFT calculations the total number of n_1 states is $n_1^{(\mathrm{tot})} = 25$. The field strength is $F = 640$ V/cm.

Our calculations do confirm, however, one example of difficulty with the local frame transformation theory that was pointed out by Zhao *et al.*, specifically Fig. 5(c) of Ref. [5] is presented in Fig. 3. We use the same parameters as in Fig. 2, and the total number of n_1 states is set to $n_1^{(\mathrm{tot})} = 25$. Here the FT-irregular function for $\ell = 6$ (red dots) does not exhibit the same convergence to the exact irregular Coulomb function as was observed for the case of $\ell = 1$ in Fig. 2(c). The biggest discrepancies occur in classically forbidden region, namely, 10 a.u. $< r <$ 25 a.u. Such a high-ℓ state is unusual because most of the disagreement shown in this comparison (see Fig. 3) resides in a classically forbidden range of r; hence the solutions plotted are testing the LFT in a region not typically expected to have strong excitation.

The study by Ref. [5] has thus been useful in pointing out that regimes, such as the $\ell = 6$ case exist where the LFT irregular function is inaccurate. Nevertheless it should be kept in mind that those discrepancies for high ℓ are nearly always unimportant because such states for any atom in the periodic table are associated with negligible quantum defects, whereby the irregular function plays virtually no role since it is always multiplied by $\sin \pi\mu_\ell$.

To summarize, the Harmin-Fano theory does not show the inaccuracies claimed by Zhao *et al.*, and the LFT is sufficiently accurate to describe the differential cross section of an alkali atom in the presence of an external electric field. Our calculations further show that the crucial element of the LFT theory, namely, the frame transformation of the irregular function in Eq. (2) accurately predicts the correct Coulomb irregular function in the field-free zone, namely, close to the origin. Furthermore, one factor that can restrict the accuracy of Eq. (2) has been demonstrated in our study, namely, the limited number of n_1 states that contribute to the summation because of the restriction of β_{n_1} to the range of $0 < \beta_{n_1} < 1$. This limitation is sufficiently accurate for low-ℓ states, e.g., with $\ell \leqslant 2$, but needs to be improved if any application is sensitive to the small-r irregular function for high ℓ, such as the $\ell = 6$ example considered here and by Zhao *et al.*

ACKNOWLEDGMENTS

This work was supported by the US Department of Energy, Office of Science, Basic Energy Sciences, under Awards No. DE-SC0010545 (for P.G. and C.H.G.) and No. DE-SC0012193 (for F.R.). We also thank L. B. Zhao, I. I. Fabrikant, M. L. Du, and C. Bourdas for discussions on the these issues.

[1] D. A. Harmin, Phys. Rev. A **26**, 2656 (1982).
[2] D. A. Harmin, Phys. Rev. Lett. **49**, 128 (1982).
[3] D. A. Harmin, Phys. Rev. A **24**, 2491 (1981).
[4] U. Fano, Phys. Rev. A **24**, 619 (1981).
[5] L. B. Zhao, I. I. Fabrikant, M. L. Du, and C. Bordas, Phys. Rev. A **86**, 053413 (2012).
[6] P. Giannakeas, F. Robicheaux, and C. H. Greene, Phys. Rev. A **91**, 043424 (2015).
[7] L. Zhao *et al.* (private communication). The energy in Fig. 5 of Ref. [5] should be $\epsilon = -135.8231$ cm^{-1}.